Peer Community Journal

Section: Plants

Research article

Published
2026-09-28

Cite as
Claire Populus, Anders Mårell and Nathalie Korboulewsky (2026) *Allometric scaling relationships of biomass for six common understory species in French temperate forests*, Peer Community Journal, 6: e100.

Correspondence
anders.marell@inrae.fr

Peer-review
Peer reviewed and recommended by PCI Plants, https://doi.org/10.24072/pci.plants.100072

Allometric scaling relationships of biomass for six common understory species in French temperate forests

Claire Populus [1], Anders Mårell [1], and Nathalie Korboulewsky [1]

Volume **6** (2026), article e100

https://doi.org/10.24072/pcjournal.806

Abstract

Forest ecologists often focus on trees and tend to overlook understory plants. However, understory species, despite representing less aboveground biomass than trees, are essential for forest dynamics and ecosystem functioning. The understory contributes to forest biodiversity, influences the forest microclimate and the availability of water and nutrients, and how disturbances, such as fires and large herbivores, impact the ecosystem. Estimating plant biomass can be difficult and time-consuming, but it is crucial to understanding and managing forest ecosystem services and risks. In this study, we improved biomass measurement methods for six common understory species in European temperate forests and with diverse ecologies and life forms: wood anemone (*Anemone nemorosa*), common heather (*Calluna vulgaris*), common honeysuckle (*Lonicera periclymenum*), purple moor-grass (*Molinia caerulea*), common bracken (*Pteridium aquilinum*) and brambles (*Rubus fruticosus* agg.). Based on vegetation samples and measurements from temperate forests in France, mostly on acidic soils, we developed aboveground biomass models. Our findings demonstrate that simple, rapid, non-destructive measurements – like cover and height – enabled us to accurately and precisely estimate the total aboveground (M_T), leaf (M_L), and stem (M_S) biomass. M_L and M_S scaled isometrically for heather and honeysuckle, and nearly isometrically for bracken, while bramble M_L and M_S scaled to 0.8 (i.e., varying leaf-to-stem ratio). These allometric scaling relationships are applicable at the scale of temperate acidic French forests and may also be applicable to European forests for the six species studied, thus promising a more complete estimation of forest biomass dynamics.

[1] INRAE, EFNO, F-45290, Nogent-sur-Vernisson, France

Peer Community Journal is a member of the Centre Mersenne for Open Scientific Publishing
http://www.centre-mersenne.org/

e-ISSN 2804-3871

Introduction

The understory, comprising all woody and non-woody vascular plants under the tree canopy that rarely exceed two meters in height (Balandier et al., 2022a), is often overlooked despite its ecological importance to forest dynamics, carbon and nutrient stocks, and ecosystem functioning (Gonzalez et al., 2013; Haritika & Negi, 2025). The contribution of understory biomass to total forest biomass varies greatly among climatic regions and forest types (Jin et al., 2022), and is mainly influenced by the availability of resources and surrounding environmental conditions. Though the understory biomass generally accounts for less than 6% of the total biomass in temperate forests and for 3% in tropical forests (Battles, 2021; Brown, 1997; Jin et al., 2022), understory leaf biomass can be equivalent to overstory leaf biomass (Landuyt et al., 2020b). Understory plants also contribute significantly to ecosystem energy, water and nutrient fluxes (Balandier et al., 2022b), affect forest regeneration dynamics (Balandier et al., 2006), constitute habitats, food and shelter for other organisms (Landuyt et al., 2019) and are an important reservoir of forest biodiversity (Gilliam, 2007). A recent review also underlines that overstory-understory interactions are not unidirectional but act in both ways with complex pathways through the facilitation and competition for light, water, and nutrients (Balandier et al., 2022b) and interact with large-scale disturbances such as fire and large herbivores (Lecomte et al., 2024) to govern species coexistence and ecosystem dynamics.

Thanks to its multiple ecological functions, the understory is a key stratum in shaping the structure and functioning of forest ecosystems. Consequently, accurately quantifying understory attributes is essential in order to understand forest dynamics and ecological processes. Community diversity describes the understory composition, while biomass serves as a proxy for ecosystem functioning and resource availability. Thus, in studies of forest regeneration, the understory biomass has been used to quantify the vegetation that facilitates or compromises the establishment of seedlings (De Lombaerde et al., 2021). It also makes it possible to assess the quantity of fine fuels in fire risks (Lecomte et al., 2024). Moreover, in studies of biogeochemical cycles, quantifying aboveground biomass made it possible to estimate the input and stock of organic matter and nutrients (Landuyt et al., 2020a). While in some studies, the vegetation cover by species or group of species is sufficient (Thomas et al., 1999; Didham et al., 2005; Maillard et al., 2021), other studies relied on understory biomass values (Bolte, 2006). Several methods are used to estimate biomass, which differ in cost, field effort, data analysis, accuracy, species, and components of biomass required. These methods were reviewed by Catchpole & Wheeler (1992), who grouped them into direct sampling methods, calibrated visual estimation methods, and double sampling methods, as developed in the following paragraphs.

Destructive sampling is a direct sampling method that involves harvesting all vegetation to measure biomass. The advantage of this method is its accuracy, as it is a direct measure of biomass at a particular sampling point. However, the sampling must be representative of the study area. This method is time-consuming and destructive, disturbing ecological processes and influencing future outcomes, especially in time-series studies. It is generally used as a reference and a calibration standard for other types of methods.

Non-destructive methods, whose main advantage is the avoidance of degrading the studied areas, are traditionally based on calibrated visual estimations (Catchpole & Wheeler, 1992). This method consists of visually estimating biomass directly *in situ*. The method requires calibration by the observer based on several quadrat samples. Qualified observers can estimate vegetation mass with an accuracy of about 90%, but efficiency and bias depend on the observer and the spatial variability of the vegetation (Catchpole & Wheeler, 1992). Another non-destructive method for estimating biomass that is less susceptible to observer effects is the point-intercept method (Jonasson, 1988), which involves recording plant contacts along vertical lines at regular intervals along a transect or within a quadrat.

The double sampling method requires only a few field samples and measurements to build allometric equations that accurately estimate biomass with minimal destruction and relatively rapid

results. Allometric equations make it possible to calculate biomass from simple and reproducible measurements. The approach is flexible and can be adapted to a wide range of ecological objectives and plant species from herbaceous species (Tackenberg, 2007; Pottier & Jabot, 2017) to trees (Bréda, 2003; Hays et al., 2020). For instance, it was used by Bréda (2003) to estimate leaf area index (LAI) in dominant trees. Several studies have developed allometric biomass models based on photographs of vegetation taken in the field followed by pixel-based image analysis (Paruelo et al., 2000; Tackenberg, 2007; Hays et al., 2020). For very large areas, biomass can be estimated from airborne LIDAR (Light Detection and Ranging) images (Estornell et al., 2011; Roth & Streit, 2018). This has the advantage of not being subject to observer effects, and allowing large areas to be covered in a short time. With a few height measurements in the field, the understory layer can be separated from the other forest strata (Ducey & Astrup, 2018). However, the calculated biomass represents the total biomass of the stratum without distinguishing among the species present, although this is a promising development direction. This method also has the disadvantage of requiring expensive equipment, and tedious and complex data processing. Field-measurements combined with allometric equations is still the most used and cheapest method, and transferable between contrasted environments (Pottier & Jabot, 2017).

In this study, allometric equations are used to calculate biomass from cover and height, or from phytovolume, combining both of these measurements (Porté et al., 2009; Pottier & Jabot, 2017). The double-sampling method can be applied to groups of understory plants (Bolte, 2006) as well as to species (Bolte, 1999; Gonzalez et al., 2013). The models for aboveground biomass estimation found in the literature were created at the local (Gonzalez et al., 2013) or regional level on different soils and types of temperate forest (Bolte, 1999, 2006).

To our knowledge, no previous studies have compared different plant cover estimation methods (i.e., two visual estimations and one systematic measurement) for biomass modelling, yet developing models for multiple cover estimation methods might add to the accuracy of the models and be useful for grouping protocols that do not use the same methods.

Besides total biomass, leaf and stem biomass and the allocation partitioning are often of interest. Separating leaf and stem biomass is essential especially for researchers attempting to model carbon and nutrient allocation (Litton et al., 2007), to study input of organic matter and nutrients to soil through litter fall (Landuyt et al., 2020a), to study the response of vegetation to biotic (herbivory) (Fan et al., 2019) or abiotic (drought, light) factors (Poorter et al., 2012), or to quantify the availability of food resources for animals (Borkowska & Konopko, 1994). Biomass allocation can be derived from the allometric partitioning theory, which is based on the metabolic scaling theory of (West et al., 1999), following the equation:

$$M_y = \alpha \cdot {M_x}^{\beta} \quad (1)$$

where M_x and M_y are the biomass of different organs, α is a species-specific normalization constant and β is the allometric scaling exponent (West et al., 1997; Enquist & Niklas, 2002). The vast majority of organisms (animals, plants, microbes) exhibit a scaling exponent very close to 0.75 according to the metabolic scaling theory. For plants, the theory was first developed and tested for tree species, confirming the theoretical scaling exponent. Then, later work showed that the exponent was equal to or very close to 1 for small or non-woody plants (Niklas, 2006). The scarcity of data on understory species is an important knowledge gap because allometric partitioning theory considers that plant size is the primary driver of biomass allocation patterns (Enquist & Niklas, 2002).

In this study, based on the double sampling method, we aim to develop models to estimate aboveground biomass (total, leaf, and stem) and provide allometric partitioning equations for leaf and stem biomass of widely represented understory plants in French and European temperate forests, with varying ecologies, botanical families and morphologies. Six species were thus sampled: wood anemone (*Anemone nemorosa* L.), common heather (*Calluna vulgaris* (L.) Hull), common honeysuckle (*Lonicera periclymenum* L.), purple moor-grass (*Molinia caerulea* (L.)

Moench), common bracken (*Pteridium aquilinum* (L.) Kuhn) and brambles (*Rubus fruticosus* agg. L.).

The objectives of the study were to:

1. Create straightforward and reproducible allometric biomass models based on parameters that are easily measured *in situ*, including cover and height.
    a. Determine the best allometric equation for each species.
    b. Determine the most accurate of the three different plant cover estimation methods.
2. Determine the constant α and the allometric scaling exponent β in the allometric partitioning equations and assess the leaf-to-stem ratio.

Materials and methods

Study sites

The 21 study sites were located in both lowland (14 sites) and mountainous (7 sites) areas in France, with altitudes ranging from 55 m to 300 m for the lowland sites and from 700 m to 1300 m for the mountain sites. The forest stands were dominated by sessile oak (*Quercus petraea* (Matt.) Liebl.) in the lowlands and silver fir (*Abies alba* Mill.) in the mountains (Table 1 and Figure 1). Oak stands were 121 ± 26 years old, and silver fir stands were 117 ± 21 years old. Most of the forest stands were managed as even-aged high forests, while some were managed as coppice with standards or uneven-aged forests. Stand basal area was calculated from tree inventory data using diameter at breast height measurements. Stand age was estimated by dendrochronological analysis (tree core sampling) from a subsample of overstory trees within each stand (see footnotes in Table 1). The study sites were located on various soil types, from extremely to slightly acidic soils, classified according to the World Reference Base soil classification system (IUSS Working Group WRB, 2015) (Table 1). Soil pH was measured in systematic and representative soil samples in the first 10 cm of the mineral soil. All the sites were located in the temperate climate zone: in the mountain sites, the mean annual temperature ranged between 6.3 and 9.8°C and the annual precipitation between 1108 and 1723 mm, while in the lowland the annual mean temperature ranged between 10.2 and 12.0°C and the annual precipitation between 707 and 1032 mm (Table 1).

Sampling of studied understory species

We studied six understory species that are common and widespread in European temperate forests, representing different morphological, biological and ecological characteristics (Table 2): *Anemone nemorosa* L. (wood anemone), *Calluna vulgaris* (L.) Hull (common heather), *Lonicera periclymenum* L. (common honeysuckle), *Molinia caerulea* (L.) Moench (purple moor-grass), *Pteridium aquilinum* (L.) Kuhn (common bracken) and *Rubus fruticosus* agg. L. (brambles). These six species are widespread, occupying over more than 50% of the European territory (Grime et al., 2007): 74% for *A. nemorosa*, 77% for *C. vulgaris and M. caerulea,* 49% for *L. periclymenum*, 92% for *P. aquilinum* and 87% for *R. fruticosus* agg.

For *R. fruticosus* agg. and the climbing species *L. periclymenum,* tall shrubs and trees were avoided and only creeping plants or those climbing on other low-growing understory plant species.

Following a visual pre-assessment of plant cover at study sites, quadrats were strategically placed to capture the full range of cover gradients present at each site. At each site, quadrats were spaced at least five meters apart to reduce spatial autocorrelation. In this way, we ensured a complete coverage of plant cover (from 1% to almost 100%) and heights across study sites and forest types. At sites 9, 13 and 19, we measured and took ten samples of *C. vulgaris, M. caerulea*, and *P. aquilinum*, and 30 samples of *A. nemorosa, L. periclymenum,* and *R. fruticosus* agg. For logistical reasons, we were unable to conduct the same sampling effort at the other sites, and reduced to four samples of each species when present and sometimes less when small and scattered presence. In total, we obtained 42 samples of *A. nemorosa*, 16 of *C. vulgaris,* 75 of *L.*

periclymenum, 27 of *M. caerulea,* 45 of *P. aquilinum*, and 103 of *R. fruticosus* agg. (Figure 1 and Table 3).

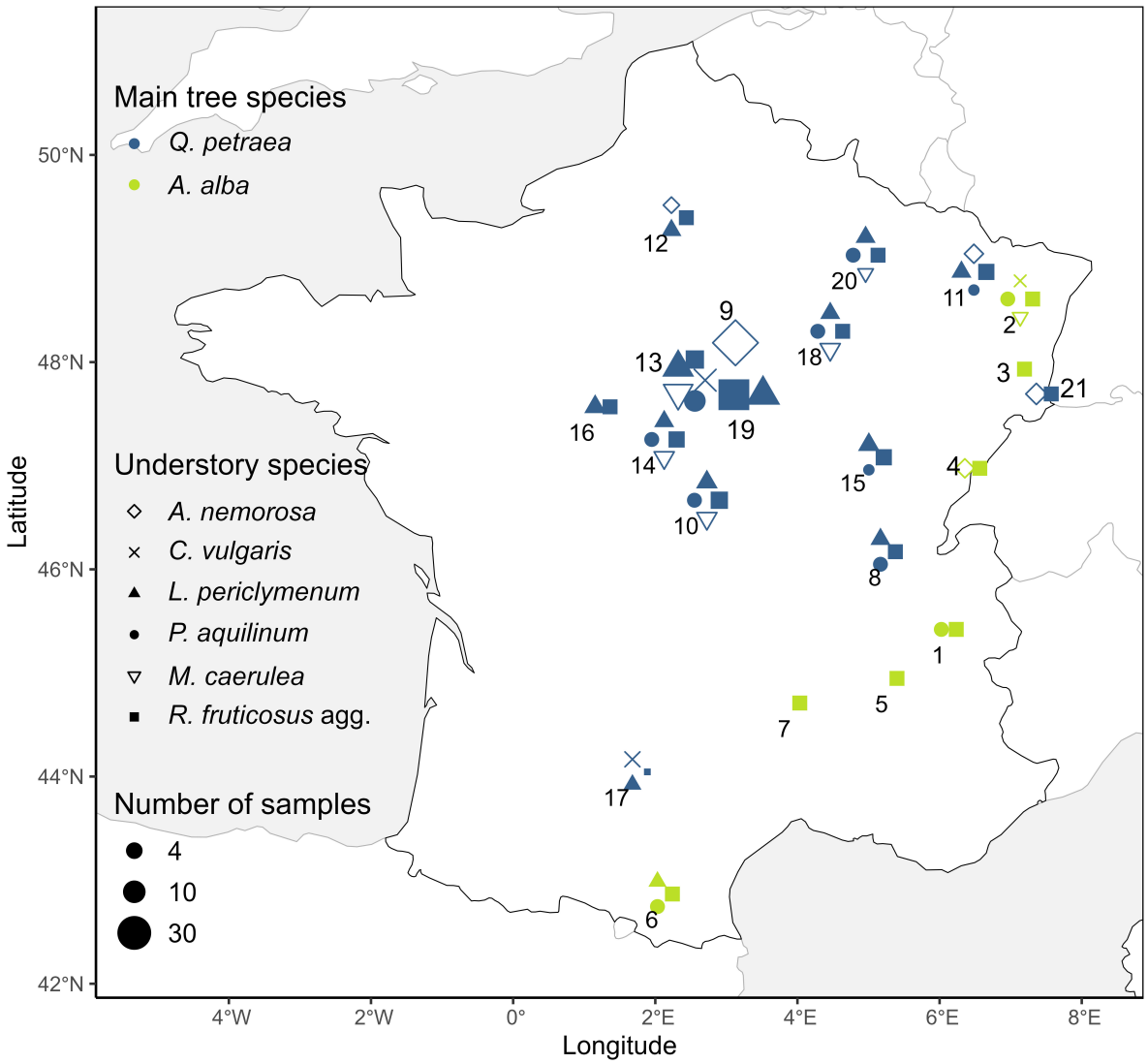

Figure 1 - Sampling design of the study. The sites (numbered from 1 to 21, Table 1) are located with symbols showing where the different understory species (*Anemone nemorosa*, *Calluna vulgaris*, *Lonicera periclymenum*, *Molinia caerulea*, *Pteridium aquilinum*, *Rubus fruticosus* agg.) were sampled. Symbol colour shows the associated type of forest: stands dominated by silver fir, *Abies alba* or sessile oak, *Quercus petraea*. Symbol size represents the number of samples per study site.

Biometrical measurements and biomass sampling of understory species

We sampled understory plants beneath forest canopies and harvested them during the peak of plant development in July and August 2023 and 2024 for *C. vulgaris*, *L. periclymenum*, *M. caerulea*, *P. aquilinum*, and *R. fruticosus* agg. (Gimingham, 1960; During et al., 1994; Taylor et al., 2001; Marrs & Watt, 2006; Taylor, 2005), and in April 2024 for *A. nemorosa* (Mårell et al., 2009). We estimated the plant cover, measured the height, and collected the living vegetative aboveground parts of the sampled plants (stems and leaves) in 0.5 m^2 quadrats (71 × 71 cm). For all measurements and sampling, only stems and leaves were taken into account and we discarded inflorescences, fruits, seeds, and dead parts.

Table 1 - Study site stand and pedo-climatic characteristics: main tree species, soil type, pH, annual mean temperature (°C), annual cumulative precipitation (mm) for the 1991-2020 period, altitude (m), forest management type, tree age (year), stand basal area (m^2 ha^{-1}) and other main tree species (in descending order of dominance and > 10% of the total basal area). NA stands for 'not available'

Forest type	Main tree species	Forest id	Soil type	pH water	Temp. (°C)	Precip. (mm)	Altitude (m)	Forest management type	Tree age (yr)	Basal area (m^2 ha^{-1})	Other main tree species
Mountain forest	*Abies alba*	1	Cambisol	4.5	7.4	1558	1100	Even-aged	123 [a]	35 [a]	-
		2		4.5	8.9	1263	400	Even-aged	83 [a]	38 [a]	*Picea abies*
		3		4.9	7.3	1611	680	Even-aged	133 [a]	49 [a]	-
		4	Cambisol and leptosol	5.7	6.3	1723	1000	Uneven-aged	110 [a]	50 [a]	*Picea abies*
		5		5.4	8.0	1371	1150	Uneven-aged	149 [a]	30 [a]	*Fagus sylvatica*
		6	Luvisol	6.2	9.8	1108	950	Even-aged	109 [a]	46 [a]	-
		7	Podzosol	4.3	6.3	1444	1300	Even-aged	109 [a]	51 [a]	-
Lowland forest	*Quercus petraea*	8	Cambisol	4.7	11.3	1032	260	Even-aged	117 [a]	31 [a]	*Carpinus betulus*
		9		5.3	11.0	707	120	Coppice with standards	105 [b]	NA	*Carpinus betulus*
		10	Cambisol and planosol	4.5	11.2	820	260	Even-aged	144 [a]	32 [a]	-
		11	Planosol	4.6	10.1	905	315	Even-aged	114 [a]	32 [a]	*Carpinus betulus*
		12		4.6	10.5	713	55	Even-aged	89 [a]	27 [a]	*Carpinus betulus*
		13		4.5	10.9	749	150	Even-aged	83 [c]	20 [c]	*Pinus sylvestris*
		14	Planosol and luvisol	4.5	11.2	834	180	Even-aged	107 [a]	30 [a]	-
		15	Luvisol	4.9	10.9	839	220	Even-aged	116 [a]	31 [a]	-
		16		4.4	11.3	669	130	Even-aged	121 [a]	34 [a]	*Fagus sylvatica*
		17		4.7	12.0	925	300	Even-aged	127 [a]	29 [a]	-
		18		4.5	10.8	803	160	Even-aged	112 [a]	26 [a]	-
		19		5.1	10.9	713	150	Coppice with standards	≈100	23 [d]	*Carpinus betulus*
		20	Podzol	4.2	10.2	892	180	Coppice with standards	168 [a]	30 [a]	*Fagus sylvatica* *Betula pendula*
		21	Calcisol	4.7	10.4	851	260	Coppice with standards	166 [a]	16 [a]	*Carpinus betulus* *Tilia cordata*

[a] Stand basal area was calculated from eight 500 m^2 subplots tree inventory data using diameter at breast height measurements. Stand age was estimated by dendrochronological analysis from a subsample of 30 overstory trees. [b] Stand age corresponded to the mean age of the sampled plots, obtained from the forest management plan. [c] Stand basal area was calculated from full tree inventory data using diameter at breast height measurements. Stand age was estimated by dendrochronological analysis from a subsample of 18 overstory trees. [d] Stand basal area was calculated from full tree inventory data using diameter at breast height measurements and including only the stems of the dominant tree species (*Quercus petraea*) with a diameter above 17.5 cm, excluding *Carpinus betulus* coppice stems.

Table 2 - Morphological characteristics, life form, life cycle and autecology of the six studied understory species

Species	Life form (Raunkiær system)	Morphology	Life cycle	Autecology
Anemone nemorosa	Geophyte	Forb. Acaulescent plant. Branched rhizome. Erect stem. Palmately lobed leaves and bracts.	Perennial. Early life cycle. Deciduous leaves.	Shade tolerance. Acidophilous to calcicolous. Mesic.
Calluna vulgaris	Chamaephyte	Dwarf shrub. Caulescent plant. Woody branched stems. Small xeromorphic leaves.	Perennial. Evergreen.	Heliophilous or partial shade. Broadly acidophilous. Xeric to hygrophilous.
Lonicera periclymenum	Chamaephyte	Shrub. Caulescent plant. Woody branched stems. Climbing or creeping twining plant. Oval hairy leaves.	Perennial. Layering. Deciduous or semi-deciduous.	Heliophilous or partial shade. Broadly acidophilous. Mesic to hygrophilous.
Molinia caerulea	Hemicryptophyte	Graminoid. Acaulescent plant. Semi-rosette tussock. Linear leaves.	Perennial. Deciduous leaves.	Heliophilous or partial shade. Acidophilous. Mesic to hygrophilous.
Pteridium aquilinum	Geophyte	Fern. Acaulescent plant. Frond arising from rhizome.	Perennial. Deciduous leaves and stem.	Heliophilous or partial shade. Broadly acidophilous. Xeric to hygrophilous.
Rubus fruticosus agg.	Phanerophytes	Shrub. Caulescent plant. Arching or erect spiny semi-woody stems. Ternate or palmate leaves.	Perennial. Layering. Biennial to perennial stems. Long-lived or persistent leaves through the winter in some taxa.	Heliophilous. Moderately acidophilous. Mesic.

Table 3 - Number of observations and descriptive statistics of projection cover (%) for each species according to forest type

Species	Forest type	Number	Min	Max	Mean	Standard deviation	Coefficient of variation
Anemone nemorosa	Lowland	39	1	98	31.6	27.8	88.0
	Mountain	3	1	8	3.7	3.8	102.7
Calluna vulgaris	Lowland	14	3	70	31.9	19.1	59.9
	Mountain	2	10	80	45.0	49.5	110.0
Lonicera periclymenum	Lowland	72	1	80	27.4	19.6	71.5
	Mountain	3	8	45	27.7	18.6	67.1
Molinia caerulea	Lowland	25	1	95	34.3	27.8	81.0
	Mountain	2	5	30	17.5	17.7	101.1
Pteridium aquilinum	Lowland	34	2	100	46.4	29.8	64.2
	Mountain	11	25	100	61.6	29.3	47.6
Rubus fruticosus agg.	Lowland	75	2	95	33.7	25.5	75.7
	Mountain	28	9	100	55.9	30.2	54.0

Plant cover

On field, we estimated three type of plant cover by (a) visual estimations of the plant cover envelope (coarse outline of the plant), (b) visual estimations of the projected plant cover (exact outline of the plant), and (c) systematic measurements following the point-intercept method using a metal rod of 4 mm in diameter and 36 points (Goodall, 1952) (Figure 2). For the point-intercept method, when the rod touched either the stem or a leaf, the species was noted present, whatever the number of contacts at the same point. The same observer carried out the visual estimates for all species and study sites to the nearest 5% to minimize any observer effect. The observer was trained on examples of known plant cover thanks to COVERater (Cruickshank et al., 2024).

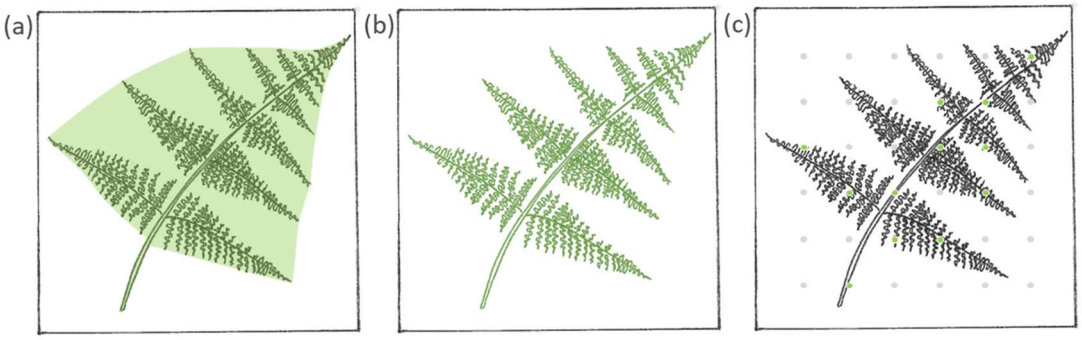

Figure 2 - Schematic representation of the three plant cover estimation methods using a triangular frond of *Pteridium aquilinum* as an example: (a) envelope, (b) projection, and (c) point-intercept method. Green areas indicate the visually estimated cover for methods (a) and (b), while the green dots in (c) represent the points in contact with the plant. For the point-intercept method, the number of contacts was converted into percentage cover using a simple proportion (e.g., 12 contacts out of 36 points correspond to a cover of 33%).

Height

For each quadrat and species, the quadrat was divided into four quarters in which we measured the height of the tallest part of the studied plant species, whether it was a stem or a leaf, using a folding ruler with centimeter precision. The maximum height was measured without straightening the plant and even if the measurements came from different parts of the same individual. We then calculated the mean among the four maximum heights per quadrat to smooth out extreme height values.

Aboveground biomass

For woody and semi-woody plants (Table 2), we sampled all living leaves and stems from inside the quadrat. We cut the aerial parts at ground level and along the vertical edges of the quadrat when plant parts extended beyond the quadrat's limits. Plant parts inside the quadrat were collected even if the plant was rooted outside. This approach was used because these species often exhibit extensive lateral branching and intertwined, layered shoots, which makes it difficult to identify the exact rooting position. Regarding herbaceous plants and ferns, we collected only those rooted within the quadrat. Thus, we collected plant parts outside the quadrat when the plant was rooted within it, and we did not collect plant parts inside the quadrat when the plant was rooted outside it. This method was preferred for herbaceous species because individual rooting points could be identified more reliably.

In the laboratory, the samples were oven-dried for 48 hours at 65°C and then weighed directly to an accuracy of 0.02 g. For the woody and semi-woody plants (*C. vulgaris*, *L. periclymenum*, *R. fruticosus* agg.), we separated the leaves (petiole included) and stems prior to oven drying. For *C. vulgaris*, as separating leaves and stems was a time-consuming task, we separated organs for only a part of each sample. To address the architectural variability observed among sites and individuals (e.g., proportion of stem and leafless parts due to age), we first separated the leafless stem sections from those with leaves. From the latter, we then defoliated 20% of the stems. This approach ensured that variability linked to architecture did not affect the subsample. Then, the leaf-to-stem mass ratio was applied to the rest of the subsample. Therefore, the leaf mass and the stem mass (sum of leafless stem and those with leaves) were obtained. For *P. aquilinum*, we separated the leaflet from the rachis of the frond, which was considered here as a stem. The total aboveground biomass was obtained by summing the dry weight of leaves and stems.

Data analysis and allometric models

Our objective was to determine the best models to estimate total (M_T), leaf (M_L), and stem (M_S) aboveground biomass from simple field measurements of plant structure. The predictors tested

included plant cover, plant height and phytovolume. Phytovolume (*P*, m^3 ha^{-1}), is a proxy of the three-dimensional space occupied by vegetation. It was calculated following Porté et al. (2009):

(2) $$P = C \cdot H$$

where *C* is the plant cover (%) and *H* is the average maximum height of the plant (cm). Models were tested separately for each species. We tested linear (Eqn. 3), second-degree polynomial (Eqn. 4), and power (Eqn. 5 and 6 used by Gonzalez et al. (2013) and Bolte (2006), respectively) scaling relationships with plant cover, average maximum height of plant or phytovolume:

(3) $$M = a \cdot v$$
(4) $$M = a \cdot v^2 + b \cdot v$$
(5) $$M = a \cdot v^b$$
(6) $$M = a \cdot C^b \cdot H^c$$

where *M is* biomass in g m^{-2}, v is any plant cover (*C*) in % or phytovolume (*P*) in m^3 ha^{-1}, *H* is the average maximum height of plant in centimeters, and *a*, *b*, and *c* are coefficients. The models were fit using the R Statistical Software (version 4.4.2).

We used weighted nonlinear least squares to fit scaling relationships between biomass and the allometric metrics (plant cover, height, and phytovolume) in order to adjust for the unbalanced sampling design (weighted proportionally to the number of quadrats per species and per study site) and to correct for heteroscedasticity, this means reducing the disproportionate influence of the most variable observations (*weights* argument in *nlsLM* function, minpack.lm R package, Elzhov et al., 2023). We ran five types of weights for each model: (i) the weight for sampling design alone, (ii) the weight for sampling design and the inverse response (a higher biomass results in a lower weight), (iii) the inverse fitted (less impacted by outliers and a higher biomass results in a lower weight), (iv) the inverse squared fitted (less impacted by outliers and a higher biomass results in a much lower weight), or (v) the inverse squared residuals (a variable biomass results in lower weight). We therefore tested and compared 21 models per species (7 scaling relationships × 3 cover methods) across the five types of weights, resulting in a total of 105 models per species and compartment (total aboveground, leaf, stem). To assess the best model and best cover methods for each species, we used three sequential criteria. (1) First, we retained the models that obeyed the hypotheses of normality of residuals and homoscedasticity using the Shapiro and the Breusch-Pagan tests at p-value 0.01 (lmtest R package, Hothorn et al., 1999), as this provides an objective and reproducible statistical evaluation compared with subjective visual inspection. (2) Then, we selected the best models based on the AICc (Akaike Information Criterion, corrected for small sample sizes). (3) Finally, when differences in AICc were lower than two, indicating models of similar explicative support, among the most parsimonious models, we chose the model with the lowest MSE (mean square error). AICc indicates the accuracy and simplicity of the model, while MSE evaluates its precision. We calculated the MAE (mean absolute error) and RMSE (root mean square error) to assess the models' predictive ability. For the best model for each species, confidence intervals of the predictions were estimated using bootstrapping (n = 1000; modelr R package, Wickham, 2023).

As site and bioclimatic conditions varied greatly among the two forest types, we expected the latter to be a discriminating covariate. We therefore also tested the effect of forest type on *a*, *b* and *c* coefficients in the best aboveground biomass models retained for species with sufficient and balanced sample sizes in both forest types, specifically *P. aquilinum* and *R. fruticosus* agg. (Table 3). More specifically, forest type was introduced as an interaction term on each coefficient (*a*, *b* and *c* when applicable), allowing each coefficient to vary between mountain and lowland forests. To select the best model (with or without forest type) we used the same criteria as for selecting the best biomass models.

To compare prediction errors (RMSE) among the three cover methods, we retained all aboveground biomass models that showed satisfactory residual patterns as identified through graphical inspection, even when the Shapiro test indicated slight deviations from normality. Indeed,

because this test is very restrictive and is sensitive to sample size, it may reject models with visually acceptable residuals distribution. Graphical inspection was therefore considered to evaluate the practical relevance of deviations from normality. Moreover, linear model coefficients and predictions are generally robust with moderate departures from normality, whereas statistical inference values such as p-values and confidence intervals are more strongly affected (Schmidt & Finan, 2018).

Here, we stipulated that the total aboveground biomass was the sum of leaf and stem biomass, $M_T = M_L + M_S$. Because it has been shown that biomass allocation patterns obey the allometric scaling law of the form $M_y = \alpha \cdot {M_x}^{\beta}$, where M_x and M_y are biomass of different organs, α is a species-specific normalization constant, and β is the allometric scaling exponent (West et al., 1997; Enquist & Niklas, 2002), we estimated the scaling exponents between leaf (M_L) and stem (M_S) biomass for the different species as follows:

(7) $$M_{Li} = \alpha_i \cdot {M_{Si}}^{\beta_i} \leftrightarrow \log_{10} M_{Li} = \log_{10} \alpha_i + \beta_i \cdot \log_{10} M_{Si}$$

and tested for differences in the scaling exponents among species, *i*, using log-log linear relationships (Eqn. 7) and standardized major axis (SMA) regression analysis (smatr R package, Warton et al., 2012). For species with a scaling exponent equal to one (β = 1, for spermatophytes without or with few secondary tissues (Niklas, 2006)), the leaf-to-stem ratio is equivalent to the constant α for each species. Since $M_T = M_L + M_S$ and $M_L = \alpha \cdot {M_S}^{\beta}$ when β = 1, simple algebraic rearrangements allow leaf and stem biomass to be estimated from the total aboveground biomass as follows:

(8) $$M_L = \frac{\alpha}{1+\alpha} \cdot M_T$$

(9) $$M_S = \frac{1}{1+\alpha} \cdot M_T$$

where α is the constant from Eqn. 7 and M_T can be replaced by the fitted equations for the total aboveground biomass (Eqn. 3-6). Eqn. 8 and 9 were not directly used in the analyses, but for convenience we present them here as they allow leaf and stem biomass to be derived from total aboveground biomass (and conversely to reconstruct total biomass from its components) when β = 1.

Results

Allometric models for aboveground biomass

Biomass allometric relationships

The plant cover gradient spanned the entire range of possible values, from 1% to almost 100%, for all six species. The total aboveground biomass ranged from 0.5 to 70 g m^{-2} for *A. nemorosa*, from 5 to 403 g m^{-2} for *C. vulgaris*, from 0.5 to 117 g m^{-2} for *L. periclymenum*, from 0.8 to 171 g m^{-2} for *M. caerulea*, from 0.6 to 323 g m^{-2} for *P. aquilinum* and from 1 to 298 g m^{-2} for *R. fruticosus* agg.

The best models for total aboveground biomass were power functions of plant cover and height (Eqn. 6) for *A. nemorosa*, *L. periclymenum,* and *P. aquilinum*, power functions of phytovolume for *M. caerulea*, and a linear function (Eqn. 3) of phytovolume for *C. vulgaris* and *R. fruticosus* agg. (Figure 3 and Table 4). All of the best models included cover and height, which were either separate variables or included in the phytovolume. Including height in these models provided precision by up to 12% for *P. aquilinum* and *R. fruticosus* agg., and between 3 and 7% for *A. nemorosa, C. vulgaris,* and *L. periclymenum*, but did not improve precision for *M. caerulea*.

Forest type had no effect on the coefficients in the model for *P. aquilinum*, but had an effect in the model for *R. fruticosus* agg.: total aboveground biomass was 9% higher in the mountain and 5% lower in the lowland than biomass estimated with the model without forest type (Appendix S1). To compare consistent models across all species, we focused on models without forest type in subsequent analyses.

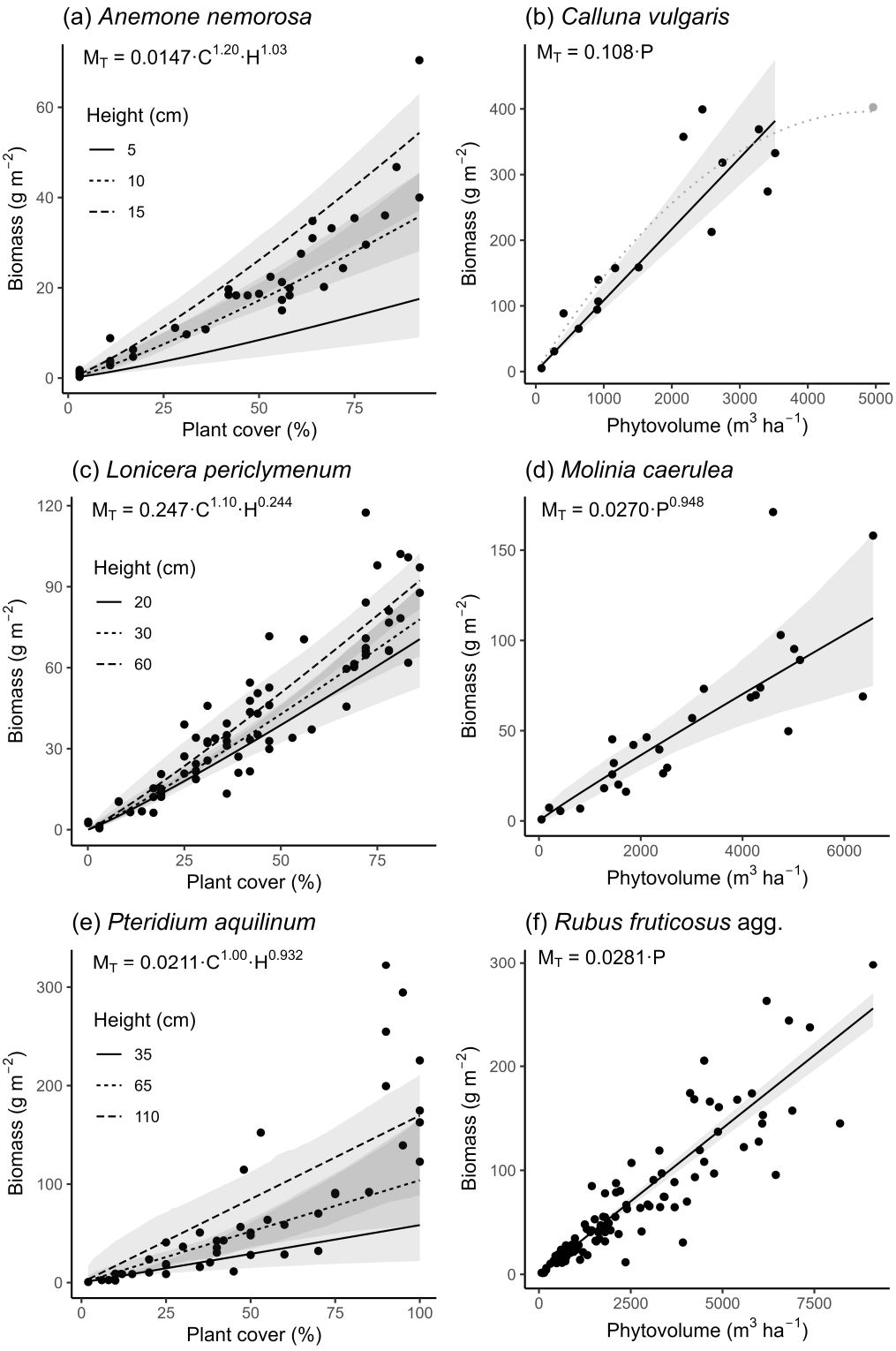

Figure 3 - Allometric relationships between total (M_T) aboveground biomass (g m^{-2}) and phytovolume (m^3 ha^{-1}) or cover (%) and height (cm) for (a) *Anemone nemorosa* (n = 42), (b) *Calluna vulgaris* (n = 16), (c) *Lonicera periclymenum* (n = 75), (d) *Molinia caerulea* (n = 27), (e) *Pteridium aquilinum* (n = 45) and (f) *Rubus fruticosus* agg. (n = 103). Points correspond to observed data, lines to model predictions, and the shaded areas to bootstrapped 95% confidence intervals. For *C. vulgaris*, the two models shown included all data (dashed gray line) or excluded (black line) an influential point (gray point). For models including height as explanatory variable, model predictions are shown for three quantiles of height (10%, 50% and 90%).

Table 4 - Best models for the allometric scaling relationship between total aboveground biomass (g m^{-2}) for six species, as well as stem and leaf biomass for four species, and phytovolume (*P* in m^3 ha^{-1}) or cover (*C* in %) and height (*H* in cm). M_T = total aboveground biomass, M_L = leaf biomass, M_S = stem biomass. Cover measure method, coefficients *a*, *b*, and *c* of the model, and p-value are given, as well as summary statistics

Formula	Cover	*a*	*b*	*c*	p-value *a*	p-value *b*	p-value *c*	Adjusted R^2	MSE	MAE	RMSE
Anemone nemorosa											
$M_T = aC^bH^c$	Point-intercept	0.0145	1.20	1.04	0.00049	<0.0001	<0.0001	0.88	25.80	3.68	5.08
Calluna vulgaris											
$M_T = aP$	Projection	0.108	-	-	<0.0001	-	-	0.79	3384	40.1	58.1
$M_L = aC + bC^2$	Projection	2.48	-0.0131	-	<0.0001	<0.0001	-	0.36	498.1	17.8	22.3
$M_S = aP$	Envelope	0.0514	-	-	<0.0001	-	-	0.79	1765	30.1	42.0
Lonicera periclymenum											
$M_T = aC^bH^c$	Point-intercept	0.247	1.10	0.244	0.0038	<0.0001	0.011	0.86	108.4	7.67	10.4
$M_L = aC^bH^c$	Point-intercept	0.146	1.09	0.119	0.0053	<0.0001	0.24	0.83	17.25	3.03	4.15
$M_S = aC^bH^c$	Point-intercept	0.112	1.13	0.305	0.012	<0.0001	0.0059	0.79	69.65	5.94	8.35
Molinia caerulea											
$M_T = aP^b$	Envelope	0.027	0.948	-	0.0079	<0.0001	-	0.66	574.5	14.6	24.0
Pteridium aquilinum											
$M_T = aC^bH^c$	Projection	0.0211	1.00	0.932	0.19	<0.0001	0.0027	0.79	1330	21.9	36.5
$M_L = aC^bH^c$	Projection	0.0159	1.47	0.473	<0.0001	<0.0001	<0.0001	0.74	721.3	15.8	26.9
$M_S = aP^b$	Projection	0.00302	1.04	-	0.022	<0.0001	-	0.79	155.3	6.94	12.5
Rubus fruticosus agg.											
$M_T = aP$	Envelope	0.0281	-	-	<0.0001	-	-	0.81	740.1	17.6	27.2
$M_L = aC + bC^2$	Point-intercept	0.240	0.00641	-	<0.0001	<0.0001	-	0.85	124.7	7.81	11.2
$M_S = aC^bH^c$	Projection	0.0132	0.836	1.22	0.0085	<0.0001	<0.0001	0.76	294.8	10.1	17.2

https://doi.org/10.24072/pcjournal.806

Cover estimation methods for biomass prediction

The best models included either point-intercept, projection, or envelope methods for estimating plant cover, depending on the species (Table 4). The best models for *C. vulgaris* and *P. aquilinum* were fitted using the projection cover, *M. caerulea* and *R. fruticosus* agg. using the envelope cover, and *A. nemorosa* and *L. periclymenum* using the point-intercept method. In this study, the three methods produced closely correlated cover estimates. The estimates of plant cover by envelope (Figure 2 (a)) and the point-intercept method (Figure 2 (c)) correlated with a unit-to-unit slope more closely (Pearson's $\rho_{a,c}$ = 0.95) than with projection (Figure 2 (b)) ($\rho_{a,b}$ = 0.94 and $\rho_{c,b}$ = 0.91, respectively) for which the slopes deviated from one.

Based on the best model for each species (Table 4), the other cover estimation methods are compared in Table 5 (for other total aboveground models, Appendix S2 and for leaf and stem models, Appendix S3). The differences in RMSE among cover methods were generally limited for *R. fruticosus* agg., *L. periclymenum* and *P. aquilinum*, with prediction errors differing by less than 10% between methods. In contrast, larger differences were observed for the other species, particularly for *C. vulgaris* and *M. caerulea,* for which the projection cover method produced lower RMSE values, with a reduction of up to 16% and 35%, respectively, compared with the envelope or point-intercept method. Considering all the models with visually satisfactory residual distributions, for each species and scaling relationship, comparisons among cover methods showed that 57% of models differed by less than 10% in prediction error, while 85% differed by less than 20% (Appendix S2).

The time to measure the visual envelope and projection cover was approximately one minute, while the time to measure the cover using the point-intercept method was around three to six minutes for the 36 points (depending on the cover, and included the phase of installing the point-quadrat).

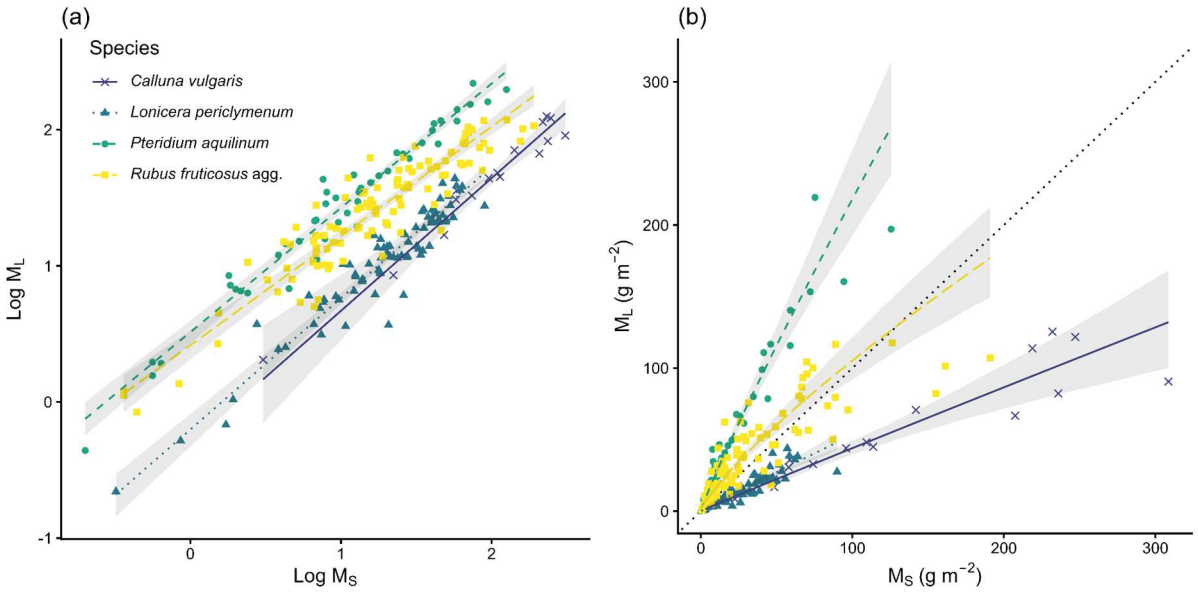

Figure 4 - Allometric relationships between leaf, M_L, and stem, M_S, biomass (g m^{-2}) for the following understory species: *Calluna vulgaris* (n = 16), *Lonicera periclymenum* (n = 75), *Pteridium aquilinum* (n = 45), and *Rubus fruticosus* agg. (n = 103). Reduced standardized major axis regression analysis of log10-transformed data (a) and back-transformed data (b). Points correspond to observed data, lines to model predictions, and the shaded areas to bootstrapped 95% confidence intervals.

Leaf-to-stem ratio

We investigated the leaf-to-stem ratio for *C. vulgaris*, *L. periclymenum*, *R. fruticosus* agg. and *P. aquilinum*. For *P. aquilinum*, the rachis was considered a stem, and the leaflets were considered leaves. The scaling exponents (β) for leaf (M_L) against stem (M_S) biomass were similar for *C. vulgaris* and *L. periclymenum* and did not differ from the expected isometric relationship ($\beta = 1$) (Figure 4 and Table 6). For these species, the coefficient α therefore represents the leaf-to-stem ratio, which remains constant regardless of the plant biomass. Contrarily, the scaling exponents for *P. aquilinum* and *R. fruticosus* agg., were below one and differed from the other species (Table 6). Consequently, the leaf-to-stem ratio was not constant and varied with plant biomass. For *R. fruticosus* agg. the scaling exponent was 0.8 which is close to the expected theoretical 0.75.

Similar patterns were observed between leaf and total aboveground biomass, and between stem and total aboveground biomass. Isometric relationships were found for most species, whereas *R. fruticosus* agg. showed a lower scaling exponent for leaf biomass and a higher scaling exponent for stem biomass with increasing total biomass. *P. aquilinum* also showed a slight increase in stem biomass allocation with increasing total biomass (Table 6).

In *L. periclymenum* and *C. vulgaris*, leaf biomass was lower than stem biomass ($\alpha < 1$). Leaf biomass represented respectively 37% and 32% of the total aboveground biomass, corresponding to a constant leaf-to-stem ratio of 0.63 and 0.50, calculated directly from the measured biomass data M_L and M_S (equivalent to the constant α when $\beta = 1$, Table 6). For *P. aquilinum*, leaf biomass was greater than rachis biomass. It varied from 76% to 68% over the range of the sampled total aboveground biomass corresponding to a leaflet-to-rachis ratio varying from 2.1 to 3.2, also derived from observed biomass. For *R. fruticosus* agg., leaf biomass was greater than stem biomass at low values of total aboveground biomass (< 224 g m^{-2}), while the inverse for higher values of total aboveground biomass (> 224 g m^{-2}) (Figure 4). The leaf-to-stem ratio varied from 0.90 to 2.57 for *R. fruticosus* agg. over the range of the studied total aboveground biomass values.

Table 5 - Allometric scaling relationships for the six studied species between aboveground biomass (M_T in g m^{-2}) and cover (C in %), height (H in cm) or phytovolume (P in m^3 ha^{-1}) following normality of residuals and homoscedasticity (Shapiro test and Breusch-Pagan test p-values (in bold) or retained following visual inception of residual patterns). The cover measure method, coefficients a, b and c of the model and p-value are given, as well as R^2, MSE, MAE, RMSE and AICc

Formula	Cover	*a*	*b*	*c*	p-value *a*	p-value *b*	p-value *c*	AICc	Adjusted R^2	MSE	MAE	RMSE	p-value Shapiro test	p-value Breusch-Pagan test
Anemone nemorosa														
$M_T = aC^bH^c$	**Point-intercept**	**0.0145**	**1.20**	**1.04**	**0.00049**	**<0.0001**	**<0.0001**	**203.2**	**0.88**	**25.80**	**3.68**	**5.08**	**0.021**	**0.14**
$M_T = aC^bH^c$	Projection	0.115	0.938	0.729	0.065	<0.0001	0.00087	247.2	0.86	29.69	3.66	5.45	0.29	0.047
$M_T = aC^bH^c$	Envelope	0.222	1.07	0.161	0.079	<0.0001	0.48	223.0	0.83	37.80	3.63	6.15	0.64	0.18
Calluna vulgaris														
$M_T = aP$	**Projection**	**0.108**	**-**	**-**	**<0.0001**	**-**	**-**	**147.0**	**0.79**	**3384**	**40.1**	**58.2**	**0.032**	**0.59**
$M_T = aP$	Envelope	0.072	-	-	<0.0001	-	-	177.3	0.73	4291	43.2	65.5	0.075	0.93
$M_T = aP$	Point-intercept	0.0624	-	-	<0.0001	-	-	182.0	0.70	4694	49.1	68.5	0.0003	0.45
Lonicera periclymenum														
$M_T = aC^bH^c$	**Point-intercept**	**0.247**	**1.10**	**0.244**	**0.0038**	**<0.0001**	**0.011**	**566.2**	**0.86**	**108.4**	**7.67**	**10.4**	**0.094**	**0.025**
$M_T = aC^bH^c$	Envelope	0.231	0.888	0.479	<0.0001	<0.0001	<0.0001	582.6	0.82	136.4	8.54	11.7	0.091	0.55
$M_T = aC^bH^c$	Projection	0.806	0.628	0.532	0.0055	<0.0001	<0.0001	601.7	0.83	126.1	8.34	11.2	<0.0001	0.33
Molinia caerulea														
$M_T = aP^b$	**Envelope**	**0.027**	**0.948**	**-**	**0.0079**	**<0.0001**	**-**	**197.4**	**0.66**	**574.5**	**14.6**	**24.0**	**0.033**	**0.42**
$M_T = aP^b$	Projection	0.0863	0.863	-	0.28	<0.0001	-	241.7	0.85	248.7	10.7	15.8	0.01	0.019
$M_T = aP^b$	Point-intercept	0.043	0.899	-	0.37	<0.0001	-	242.3	0.65	595.6	15.9	24.4	0.013	0.37
Pteridium aquilinum														
$M_T = aC^bH^c$	**Projection**	**0.0211**	**1.00**	**0.932**	**0.19**	**<0.0001**	**0.0027**	**406.7**	**0.79**	**1330**	**21.9**	**36.5**	**0.022**	**0.10**
$M_T = aC^bH^c$	Point-intercept	0.000484	1.97	0.789	0.57	0.0002	0.0017	448.9	0.79	1326	22.9	36.4	<0.0001	0.056
$M_T = aC^bH^c$	Envelope	0.0003	1.55	1.26	0.45	0.0002	<0.0001	418.3	0.75	1529	23.3	39.1	0.0027	0.21
Rubus fruticosus agg.														
$M_T = aP$	**Envelope**	**0.0281**	**-**	**-**	**<0.0001**	**-**	**-**	**858.4**	**0.81**	**740.1**	**17.6**	**27.2**	**0.13**	**0.95**
$M_T = aP$	Point-intercept	0.0296	-	-	<0.0001	-	-	875.5	0.79	799.1	18.0	28.3	0.033	0.21
$M_T = aP$	Projection	0.0331	-	-	<0.0001	-	-	769.7	0.82	681.3	17.6	26.1	<0.0001	0.038

https://doi.org/10.24072/pcjournal.806

Table 6 - Summary statistics of the reduced standardized major axis regression analysis of log10-transformed data for total above (M_T), leaf (M_L), and stem (M_S) biomass (g m^{-2}). Scaling parameters of models α and β are given, as well as the adjusted R^2 and the p-values the test of the scaling exponent β against the theoretical values of 1 and 0.75. * indicates that β was not significantly different from 1 and † indicates that β was not significantly different from 0.75. Differences in the scaling exponent β between species are indicated by a different letter (post-hoc pair-wise comparisons with Sidak correction, *sma* function, smatr R package, Warton et al., 2012)

Species	Log10 α (95% CI)	α (95% CI)	β (95% CI)	p-value (β = 1)	p-value (β = 0.75)	Post-hoc test	Adjusted R^2
M_L versus M_S							
Calluna vulgaris	-0.30 (-0.62; 0.011)	0.50 (0.24; 1.03)	0.97 (0.83; 1.14)*	0.73	0.003	ab	0.96
Lonicera periclymenum	-0.20 (-0.32; -0.087)	0.63 (0.48; 0.82)	0.96 (0.89; 1.05)*	0.41	<0.0001	b	0.90
Pteridium aquilinum	0.51 (0.44; 0.59)	3.24 (2.75; 3.89)	0.91 (0.85; 0.98)	0.009	<0.0001	ab	0.96
Rubus fruticosus agg.	0.42 (0.32; 0.50)	2.63 (2.09; 3.16)	0.80 (0.74; 0.87)†	<0.0001	0.12	a	0.86
M_L versus M_T							
Calluna vulgaris	-0.50 (-0.74; -0.25)	0.32 (0.18; 0.56)	0.99 (0.89; 1.11)*	0.9	<0.0001	a	0.98
Lonicera periclymenum	-0.43 (-0.52; -0.34)	0.37 (0.30; 0.46)	0.99 (0.93; 1.05)*	0.7	<0.0001	a	0.96
Pteridium aquilinum	-0.11 (-0.14; -0.073)	0.78 (0.72; 0.85)	0.98 (0.96; 1.00)*	0.02	<0.0001	a	0.99
Rubus fruticosus agg.	-0.12 (-0.18; -0.054)	0.76 (0.66; 0.88)	0.93 (0.90; 0.97)	0.0005	<0.0001	a	0.97
M_S versus M_T							
Calluna vulgaris	-0.20 (-0.31; -0.09)	0.63 (0.49; 0.81)	1.02 (0.97; 1.07)*	0.5	<0.0001	a	0.99
Lonicera periclymenum	-0.24 (-0.29; -0.19)	0.58 (0.51; 0.65)	1.03 (0.99; 1.06)*	0.1	<0.0001	a	0.99
Pteridium aquilinum	-0.68 (-0.76; -0.59)	0.21 (0.17; 0.26)	1.07 (1.02; 1.12)	0.006	<0.0001	ab	0.98
Rubus fruticosus agg.	-0.66 (-0.75; -0.57)	0.22 (0.18; 0.27)	1.15 (1.10; 1.21)	<0.0001	<0.0001	b	0.96

https://doi.org/10.24072/pcjournal.806

Discussion

Allometric models for aboveground biomass

Species-specific allometric relationships for aboveground biomass

We developed allometric models based on simple, rapid, and non-destructive field measurements for six understory species that are widespread in European temperate forests and exhibit different morphologies, ecologies and life cycles (Objective 1.a.). These were developed for plants growing under the forest canopy across a wide range of biomass in temperate mountain and lowland forests. Nevertheless, the observed biomass range was low to medium, corresponding to under-canopy conditions. Therefore, for a broader and more generalized application of the models, they could be updated with measurements in areas with more available light, such as from open areas where these species are more developed (Gaudio et al., 2011), or by developing biomass correction factors based on light (Heinrichs et al., 2010). Indeed, the maximum biomass harvested for *C. vulgaris* and *M. caerulea* was below the values reported in the literature (Table 7). This difference in biomass between the present study and the literature was probably due to lower light available under oak and fir than under pine (Gonzalez et al., 2013) or on heathland (Aerts, 1989). The higher the light availability, the higher the tissues density, number of branches and leaf density (Poorter et al., 2019). The biomass range for *P. aquilinum* was in agreement with the mean value under pine (Gonzalez et al., 2013) but below the maximal value reported by Le Duc et al. (2000) and Gonzalez et al. (2013) (Table 7). The biomass of *A. nemorosa, L. periclymenum,* and *R. fruticosus* agg. has been rarely studied. The ranges we observed were in agreement with the biomass reported in the literature (Table 7). Forest type can be considered, as plants are subject to varying climate, soil, and stand tree species. Our results indicated that biomass models could differ slightly (i.e., *R. fruticosus* agg., with less than 10% difference), or not (i.e., *P. aquilinum*), between mountain and lowland forests in a temperate climate (Appendix S1). However, for the other species, insufficient data were available to properly test for the effect of forest type, but the models are currently robust for lowland forests. Balanced sampling across both forest types would help improve these models and increase their generality.

Table 7 - Range of total aboveground biomass (g m^{-2}) measured for each species at the study sites and in comparison with aboveground biomass values (g m^{-2}) reported in the literature

Species	Total aboveground biomass range (g m^{-2})	Aboveground biomass in the literature (g m^{-2})
Anemone nemorosa	0.5 to 70	15 (Rawlik & Jagodziński, 2022)
Calluna vulgaris	5 to 403	Up to 740 (Gonzalez et al., 2013) Up to 900 (Aerts, 1989)
Lonicera periclymenum	0.5 to 117	48 (Madgwick, 1965) 70 (During et al., 1994)
Molinia caerulea	0.8 to 171	Up to 550 (Gonzalez et al., 2013) Up to 670 (Aerts, 1989)
Pteridium aquilinum	0.6 to 323	230 in average and up to 847 (Gonzalez et al., 2013) Up to 670 (Le Duc et al., 2000)
Rubus fruticosus agg.	1 to 298	83 (Madgwick, 1965)

Best biomass models included both cover and height, whether it was the total aboveground biomass, leaf biomass, or stem biomass. Models based on phytovolume, i.e., with simultaneous changes in cover and height, were the best for the shrubs *C. vulgaris* and *R. fruticosus* agg. and the grass *M. caerulea,* while models involving independent changes in cover and height were the best for the herbaceous plants *A. nemorosa* and *P. aquilinum,* and the climbing shrub *L. periclymenum*. Several studies have proposed biomass models based only on plant cover (Röttgermann et al., 2000; Rue-Johns et al., 2021; Monzingo et al., 2022) for a cost-effective field protocol. For small-growing plants, such models can be sufficient to get a good or excellent relation (R^2 = 0.61 to 0.94 (Röttgermann et al., 2000)). Nonetheless, some authors recognized that including plant height could improve the precision of estimates (Rue-Johns et al., 2021). Moreover,

our study and others (Bolte, 2006; Gonzalez et al., 2013) have shown that statistical analysis based on model selection indicates that model fitting is better when height is included, even so for small-growing plants such as *A. nemorosa*. We also found that including height was even more important when the plant cover was high because plant height can vary significantly among sites with equivalent plant covers. We found that this was particularly the case for *P. aquilinum* and *R. fruticosus* agg., for which plant height could be either low or high at the same plant cover. Consistent with these observations, models including both cover and height more frequently showed visually satisfactory residual distributions (64%) than the models based on cover alone (46%), highlighting the contribution of height to improving model fit. For some shrub species and young tree species, height can be associated with stem diameter and age, making it a better predictor of woody biomass than cover alone (Annighöfer et al., 2016; Rue-Johns et al., 2021).

Total biomass models were either linear for *C. vulgaris* and *R. fruticosus* agg. or a power function for the four other studied species. Both similar and different model forms can be found in the literature (Bolte, 2006; Gonzalez et al., 2013). Total biomass models had the same form as for their leaf and stem biomass models, except for *C. vulgaris* and *R. fruticosus* agg., for which cover only was used in modeling leaf biomass (Table 4, Appendix S4 and Appendix S5). Leaves of *C. vulgaris* and *R. fruticosus* agg. were mainly found at the top of the shrub, regardless of the stem height. It is worth noting that the total biomass model applied to *C. vulgaris* was sensitive to the unique high phytovolume value (approximately 5000 m^3 ha^{-1}), and that the model must be used within the range for which it has been developed (phytovolume up to 3500 m^3 ha^{-1}, Figure 3 (b)).

When comparing predicted biomass from our models with those obtained using species-specific equations from Gonzalez et al. (2013) and group-level models from Bolte (2006), we found consistent discrepancies for the shared species. The allometric equations provided by Gonzalez et al. (2013) tended to overestimate the biomass at our study sites (up to 40% for *P. aquilinum*), whereas the species-grouped models of Bolte (2006) generally underestimated biomass (up to -117% for *A. nemorosa* and -94% for *P. aquilinum*). These differences further highlight that biomass models are species-specific and sensitive to ecological context. However, models can still be applied to new sites, provided that their suitability for the studied sites is first verified through a limited number of field measurements and samplings.

Comparison of cover estimation methods and practical implications

We tested three methods of measuring vegetation cover (Objective 1.b.). The most parsimonious model included different cover methods depending on the species, and we then compared these best models to the other cover methods used. Based on the model quality indicators, all three cover methods provided good predictive accuracy (Table 5 and Appendix S2). Indeed, more than 50% of the models differed by less than 10% in prediction error among cover methods, and approximately 80% differed by less than 20%.

Developing models for multiple cover methods can be useful for grouping protocols that do not use the same methods. The visual envelope and projection methods were quick to perform and applicable at any scale. The drawback is that these methods are subject to an important observer effect (Couvreur et al., 2015), but this can be minimized by calibration against references and among the observers themselves. The point-intercept method is systematic and, therefore, not subject to any observer effect. However, the diameter of the rod has an influence. The thinner the rod, the closer the point-intercept cover is to the actual projection cover, and the wider the rod, the more the cover is overestimated (Goodall, 1952). This is particularly relevant when the rod is wider, as in our case, where the cover is more closely related to the envelope cover. The estimation error with a wider rod depends on the plant's architecture which affects the probability of interception. The point-intercept method required a larger installation and took up to six times longer time to measure than visual estimation. Finally, it is worth noting that this method proved difficult to use in windy conditions. The effort of measuring height is also time-consuming, but it gave higher precision for all the six studied species.

Overall, because the three cover methods produced strongly correlated cover estimates and relatively similar predictive performances in most cases, the choice of method may depend

primarily on the study objective and field constraints. Projection cover appeared to provide the best compromise between predictive accuracy and field applicability. Although slightly more difficult to estimate visually than envelope cover, it remains rapid to measure while better representing the true plant area. In contrast, envelope cover is less precise as the definition of the outline of the vegetation depends on the observer judgement, despite being as rapid to assess as projection cover. The point-intercept method provides systematic measurements that are less dependent on the observer, but it requires more installation time and substantially longer field measurements.

Scaling relationship among leaf, stem and total biomass

Allometric partitioning theory predicts that aboveground biomass M_T should scale nearly isometrically with leaf biomass, M_L, and stem biomass, M_S (Enquist & Niklas, 2002; Niklas, 2006). Because gross photosynthesis is supposed to scale proportionally to leaf surface area and, indirectly to leaf biomass, M_L, theory predicts that the surface areas over which resources are exchanged with the environment (which correlate with M_L) scale isometrically with the total plant biomass, M_T (Enquist & Niklas, 2002; Niklas, 2006; Cheng et al., 2014). However, the relationship between leaf biomass and leaf surface area may vary among and within species due to differences in specific leaf area (SLA, Poorter et al., 2009). For spermatophytes lacking the capacity to produce secondary tissues or small plants (such as seedlings), the scaling exponent is expected to be 1. However, for spermatophytes with a high amount of secondary tissues and tall plants, M_L is expected to scale on average as the 0.75 power of both M_T and M_S (Enquist & Niklas, 2002; Niklas, 2006). We found an isometric scaling relationship between M_L and M_T, M_L and M_S, and M_S and M_T for two species studied and different from 1 for the two other species (Objective 2). The scaling exponent was not significantly different from the isometric exponent for *C. vulgaris* and *L. periclymenum*, while it was slightly diverging for *P. aquilinum* and *R. fruticosus* agg. In other words, for the two first species, the allometric partitioning remained constant throughout the biomass gradient. *R. fruticosus* agg. exhibited the lowest scaling exponent for M_L versus M_T and M_L versus M_S, indicating that the leaf-to-stem ratio varied with plant biomass. Similarly, other studies did not find exactly 1, but generally reported values between 0.80 (or even lower) and 1.16 (Cheng et al., 2015; Liu et al., 2021). If the scaling exponent used is inappropriate for the species, its predictions would be biased and the relative error in biomass estimation increases as biomass increases. The likely explanation for the coefficient differing from 1 is that plants allocate more or less resources to conducting and supporting tissues as their size (and therefore their aboveground biomass) increases (Figure 5). Although the general power model $M_L = \alpha \cdot {M_S}^{\beta}$ was significant for *R. fruticosus* agg., it is worth noting that samples for the highest biomass were distant from the predicted relationship. This may be explained by the fact that the linear log-log transformation do not always provide the best fit of data to the model (Niklas, 2006). For *R. fruticosus* agg., the tipping point (when leaf and stem biomass were equal), as determined by a linear log-log transformation was, 224 g m^{-2} of M_T, whereas it was only 92 g m^{-2} with a non-linear regression. More data are needed to better fit the model for larger biomass levels.

Despite their widespread use, allometric relationships have several important limitations and debates (Niklas, 2006). Estimated scaling exponents may be strongly influenced by phylogenetic constraints and dataset composition, limiting their generalization across taxa. In addition, parameter estimates can vary depending on the regression approach used (e.g., ordinary least squares, reduced major axis, or standardized major axis), raising questions about the biological meaning of fitted coefficients, even when numerical fits are robust. Furthermore, while isometric scaling is often assumed as a null expectation, many biological systems exhibit non-isometric scaling linked to biophysical constraints, suggesting that scaling exponents reflect more than simple proportional changes in size, underlying structural and functional constraints. These limitations are particularly relevant when interpreting species-specific allometric patterns and biomass allocation strategies, as observed in the present study.

The shrubs *C. vulgaris* and *L. periclymenum* had a leaf-to-stem ratio of less than 1, meaning that leaf biomass represented less than half of the aboveground biomass. These shrub species are perennial, and their stems play a supporting role, which explains the higher investment in stem

biomass compared to leaves (Klimeš et al., 2020). The fern (*P. aquilinum*), like most herbaceous plants, had a leaflet-to-rachis ratio greater than 1, meaning that biomass was mainly allocated to leaf development, the organ of energy production, in order to grow and develop their reserves and ensure their reproduction (Poorter et al., 2012). The bramble *R. fruticosus* agg. had a leaf-to-stem ratio > 1 when small, and < 1 when it got bigger. Small individuals invest more in leaves and as brambles grow, their stems become more numerous and taller, overlapping one another, and leaves develop primarily on the outer parts. Depending on the size of the bramble shrub, the leaf-to-stem ratio can nearly triple.

Therefore, leaf-to-stem ratio reflects a compromise between resource acquisition and structural investment. These strategies correspond to the Leaf Economics Spectrum (Wright et al., 2004), later expanded to Plant Economics Spectrum (Reich, 2014), integrating biomass allocation among plant organs. A high ratio generally illustrates an acquisitive strategy, characterized by a strong ability to capture resources and rapid growth, as commonly observed in herbaceous species, whereas a low ratio indicates a more conservative and sustainable strategy, typical of shrubs and trees. The decrease in ratio with increasing size in *R. fruticosus* agg. reflects a plasticity in biomass allocation from resource acquisition towards structural support.

Biomass allocation patterns may also vary under environmental constraints such as thermal, water, or nutrient stress, which can modify plant allometry and allocation plasticity or strategies (Poorter et al., 2012). Under stressful conditions, plants may allocate proportionally more biomass to supporting or persistent tissues at the expense of leaves in order to improve survival and resource conservation. Consequently, allometric relationships and leaf-to-stem ratio may provide useful indicators of plant ecological strategies and environmental conditions. Because leaves and stems differ in turnover rates, decomposition, and nutrient contents, biomass partitioning also influences litter production and nutrient cycling within forest ecosystems.

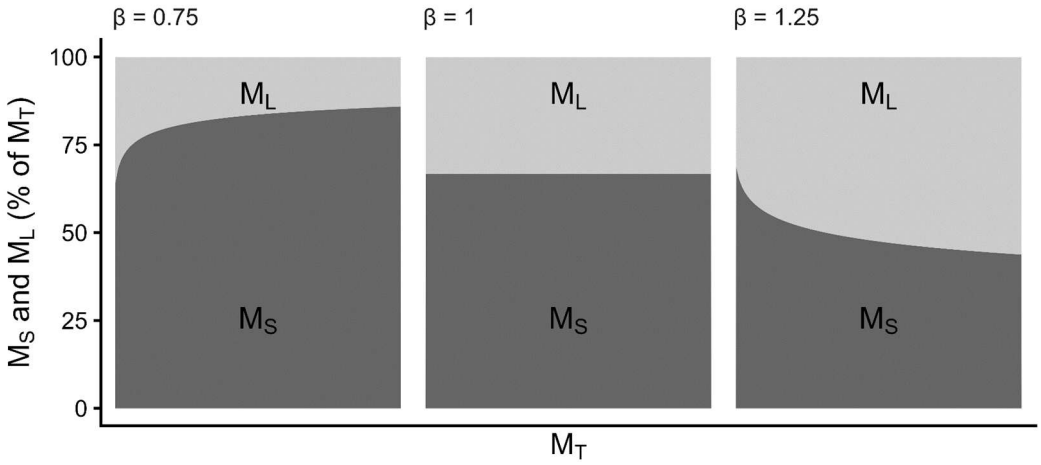

Figure 5 - Relative contributions of leaf (M_L) and stem (M_S) biomass to total aboveground biomass (M_T) across increasing M_T values and different scaling exponents β, with leaf-to-stem ratio α = 0.5 (Eqn. 7).

Conclusion

Simple, rapid, and non-destructive measurements (cover and height) enabled us to estimate the aboveground biomass of the understory accurately and precisely (adjusted R^2 > 0.65). We confirmed that adding height to cover improved the models significantly. The allometric equations developed in this study were suitable for a large range of temperate forests for the six species studied. However, they apply only to understory conditions beneath the forest canopy where total biomass is low to medium. Overall, all three cover estimation methods provided satisfactory biomass estimates, but projection cover appeared to provide the best compromise between

predictive accuracy, ecological realism and field efficiency for estimating understory biomass. Our results conform to the theory of allometric partitioning for our understory species with an isometric or near-isometric scaling relationship. Allometric equations can be useful for many studies, such as those on carbon and nutrient storage and flow, food availability for animals, or quantifying vegetation response to certain factors such as drought or herbivory.

Acknowledgments

The authors thank Camille Viguié, Aviva Kara and Jeremy Lucas for field assistance. The field was carried out on OPTMix, an experimental site of National Research Institute for Agriculture, Food and Environment (INRAE) and RENECOFOR, an experimental site of the French National Forest Office (ONF). The experimental site OPTMix (https://optmix.efno.fr/) was installed and equipped by INRAE EFNO thanks to the Centre Val-de-Loire region, the Loiret and the French National Forest Office, and belongs to networks ANAEE-F (http://www.anaee-france.fr/).
Preprint version 4 of this article has been peer-reviewed and recommended by Peer Community In Plants (https://doi.org/10.24072/pci.plants.100072; Vernay, 2026).

Funding sources

This study was partially supported by a grant from ONF “Convention de partenariat Recherche pour l’étude de l’impact des ongulés sauvages et de leur exclusion sur la stœchiométrie des écosystèmes forestiers dans le réseau RENECOFOR”.

Author contributions

Claire Populus: Data curation, Formal analysis, Investigation, Methodology, Validation, Visualization, Writing – original draft, Writing – review and editing. Anders Mårell: Conceptualization, Formal analysis, Investigation, Methodology, Supervision, Validation, Visualization, Writing – original draft, Writing – review and editing. Nathalie Korboulewsky: Conceptualization, Funding acquisition, Investigation, Methodology, Project administration, Supervision, Validation, Visualization, Writing – original draft, Writing – review and editing.

Conflict of interest disclosure

The authors declare that they comply with the PCI rule of having no financial conflicts of interest in relation to the content of the article.

Data availability statement

Data available: https://doi.org/10.57745/TEKLCI (Populus et al., 2026)
Supplementary information: https://hal.inrae.fr/hal-05527391

References

Aerts, R. (1989). Aboveground biomass and nutrient dynamics of Calluna vulgaris and Molinia caerulea in a dry heathland. Oikos, 56(1), 31. https://doi.org/10.2307/3566084

Annighöfer, P., Ameztegui, A., Ammer, C., Balandier, P., Bartsch, N., Bolte, A., Coll, L., Collet, C., Ewald, J., Frischbier, N., Gebereyesus, T., Haase, J., Hamm, T., Hirschfelder, B., Huth, F., Kändler, G., Kahl, A., Kawaletz, H., Kuehne, C., … Mund, M. (2016). Species-specific and generic biomass equations for seedlings and saplings of European tree species. European Journal of Forest Research, 135(2), 313–329. https://doi.org/10.1007/s10342-016-0937-z

Balandier, P., Gobin, R., Prévosto, B., & Korboulewsky, N. (2022a). The contribution of understorey vegetation to ecosystem evapotranspiration in boreal and temperate forests: A literature review

and analysis. European Journal of Forest Research, 141(6), 979–997. https://doi.org/10.1007/s10342-022-01505-0

Balandier, P., Mårell, A., Prévosto, B., & Vincenot, L. (2022b). Tamm review: Forest understorey and overstorey interactions: So much more than just light interception by trees. In Forest Ecology and Management (Vol. 526, p. 120584). https://doi.org/10.1016/j.foreco.2022.120584

Balandier, P., Sonohat, G., Sinoquet, H., Varlet-Grancher, C., & Dumas, Y. (2006). Characterisation, prediction and relationships between different wavebands of solar radiation transmitted in the understorey of even-aged oak (Quercus petraea, Q. robur) stands. Trees, 20(3), 363–370. https://doi.org/10.1007/s00468-006-0049-3

Battles, J. (2021). Forest biomass and primary productivity. In Online Book: A Synthesis of Scientific Research at Hubbard Brook (Hubbard Brook Research Foundation / HBR-LTER). https://hubbardbrook.org/onlhttps://hbr-lter.github.io/synthesisbook/BiomassProductivity.html

Bolte, A. (1999). Abschätzung von Trockensubstanz-, Kohlenstoff- und Nährelementvorräten der Waldbodenflora: Verfahren, Anwendung und Schätztafeln. Ulmer.

Bolte, A. (2006). Biomasse- und Elementvorräte der Bodenvegetation auf Flächen des Forstlichen Umweltmonitorings in Rheinland-Pfalz (BZE, Level II): Förder-Kennzeichen FAWF/0228/C/2/05. Selbstverl. des Forschungszentrums Waldökosysteme der Univ. Göttingen.

Borkowska, A., & Konopko, A. (1994). The winter browse supply for moose in different forest site-types in the Biebrza Valley, Poland. Acta Theriologica, 39, 67–71. https://doi.org/10.4098/AT.arch.94-8

Bréda, N. J. J. (2003). Ground-based measurements of leaf area index: A review of methods, instruments and current controversies. Journal of Experimental Botany, 54(392), 2403–2417. https://doi.org/10.1093/jxb/erg263

Brown, S. (with Food and Agriculture Organization of the United Nations). (1997). Estimating biomass and biomass change of tropical forests: A primer. Food and Agriculture Organization of the United Nations.

Catchpole, W. R., & Wheeler, C. J. (1992). Estimating plant biomass: A review of techniques. Australian Journal of Ecology, 17(2), Article 2. https://doi.org/10.1111/j.1442-9993.1992.tb00790.x

Cheng, D., Ma, Y., Zhong, Q., & Xu, W. (2014). Allometric scaling relationship between above- and below-ground biomass within and across five woody seedlings. Ecology and Evolution, 4(20), 3968–3977. https://doi.org/10.1002/ece3.1184

Cheng, D., Zhong, Q., Niklas, K. J., Ma, Y., Yang, Y., & Zhang, J. (2015). Isometric scaling of above- and below-ground biomass at the individual and community levels in the understorey of a sub-tropical forest. Annals of Botany, 115(2), 303–313. https://doi.org/10.1093/aob/mcu238

Couvreur, J.-M., Fiévet, V., Smits, Q., & Dufrêne, M. (2015). Evaluation of the “observer effect” in botanical surveys of grasslands. Biotechnology, Agronomy, Society and Environment, 19, 132–142.

Cruickshank, M. M., Moles, A. T., Debono, S. A., & Xirocostas, Z. A. (2024). COVERater—A Free Application for Training Researchers to Accurately Estimate Species Cover in Terrestrial and Aquatic Ecosystems. Ecology and Evolution, 14(10), e70447. https://doi.org/10.1002/ece3.70447

Didham, R. K., Tylianakis, J. M., Hutchison, M. A., Ewers, R. M., & Gemmell, N. J. (2005). Are invasive species the drivers of ecological change? Trends in Ecology & Evolution, 20(9), 470–474. https://doi.org/10.1016/j.tree.2005.07.006

Ducey, M. J., & Astrup, R. (2018). Rapid, nondestructive estimation of forest understory biomass using a handheld laser rangefinder. Canadian Journal of Forest Research, 48(7), Article 7. https://doi.org/10.1139/cjfr-2017-0441

During, H. J., Kwant, R. A., & Werger, M. J. A. (1994). Effects of light quantity on above-ground biomass investment patterns in the vine Lonicera periclymenum and the shrub Lonicera xylosteum. Phytocoenologia, 24(1–4), 597–607. https://doi.org/10.1127/phyto/24/1994/597

Elzhov, T. V., Mullen, K. M., Spiess, A.-N., & Bolker, B. (2023). minpack.lm: R interface to the Levenberg-Marquardt nonlinear least-squares algorithm found in MINPACK, plus support for bounds (p. 1.2-4). https://doi.org/10.32614/CRAN.package.minpack.lm

Enquist, B. J., & Niklas, K. J. (2002). Global allocation rules for patterns of biomass partitioning in seed plants. Science, 295(5559), 1517–1520. https://doi.org/10.1126/science.1066360

Estornell, J., Ruiz, L. A., Velázquez-Martí, B., & Fernández-Sarría, A. (2011). Estimation of shrub biomass by airborne LiDAR data in small forest stands. Forest Ecology and Management, 262(9), 1697–1703. https://doi.org/10.1016/j.foreco.2011.07.026

Fan, Z., Chen, B., Liao, H., Zhou, G., & Peng, S. (2019). The effect of allometric partitioning on herbivory tolerance in four species in South China. Ecology and Evolution, 9(20), 11647–11656. https://doi.org/10.1002/ece3.5651

Gaudio, N., Balandier, P., Philippe, G., Dumas, Y., Jean, F., & Ginisty, C. (2011). Light-mediated influence of three understorey species (Calluna vulgaris, Pteridium aquilinum, Molinia caerulea) on the growth of Pinus sylvestris seedlings. European Journal of Forest Research, 130(1), 77–89. https://doi.org/10.1007/s10342-010-0403-2

Gilliam, F. S. (2007). The ecological significance of the herbaceous layer in temperate forest ecosystems. BioScience, 57(10), 845–858. https://doi.org/10.1641/B571007

Gimingham, C. H. (1960). Calluna Salisb. Journal of Ecology, 48(2), 455–483. https://doi.org/10.2307/2257528

Gonzalez, M., Augusto, L., Gallet-Budynek, A., Xue, J., Yauschew-Raguenes, N., Guyon, D., Trichet, P., Delerue, F., Niollet, S., Andreasson, F., Achat, D. L., & Bakker, M. R. (2013). Contribution of understory species to total ecosystem aboveground and belowground biomass in temperate Pinus pinaster Ait. Forests. Forest Ecology and Management, 289, 38–47. https://doi.org/10.1016/j.foreco.2012.10.026

Goodall, D. (1952). Some considerations in the use of point quadrats for the analysis of vegetation. Australian Journal of Biological Sciences, 5(1), Article 1. https://doi.org/10.1071/BI9520001

Grime, J. P., Hodgson, J. G., Hunt, R., & Hunt, R. (2007). Comparative plant ecology: A functional approach to common British species (2. ed). Castlepoint Press [u.a.].

Haritika, & Negi, A. K. (2025). The underestimated role of understory vegetation dynamics for forest ecosystem resilience: A review. Plant Ecology, 226(7), 763–787. https://doi.org/10.1007/s11258-025-01529-7

Hays, B. R., Riginos, C., Palmer, T. M., Gituku, B. C., & Goheen, J. R. (2020). Using photography to estimate above-ground biomass of small trees. Journal of Tropical Ecology, 36(5), 213–219. https://doi.org/10.1017/S0266467420000139

Heinrichs, S., Bernhardt-Römermann, M., & Schmidt, W. (2010). The estimation of aboveground biomass and nutrient pools of understorey plants in closed Norway spruce forests and on clearcuts. European Journal of Forest Research, 129, 613–624. https://doi.org/10.1007/s10342-010-0362-7

Hothorn, T., Zeileis, A., Farebrother, R. W., & Cummins, C. (1999, March 15). lmtest: Testing linear regression models (p. 0.9-40). https://doi.org/10.32614/CRAN.package.lmtest

IUSS Working Group WRB. (2015). World Reference Base for Soil Resources 2014, update 2015, International soil classification system for naming soils and creating legends for soil maps. (World Soil Resources Reports No. 106). FAO.

Jin, Y., Liu, C., Qian, S. S., Luo, Y., Zhou, R., Tang, J., & Bao, W. (2022). Large-scale patterns of understory biomass and its allocation across China's forests. Science of The Total Environment, 804, 150169. https://doi.org/10.1016/j.scitotenv.2021.150169

Jonasson, S. (1988). Evaluation of the point intercept method for the estimation of plant biomass. Oikos, 52(1), Article 1. https://doi.org/10.2307/3565988

Klimeš, A., Klimešová, L., Bartušková, A., & Klimešová, J. (2020). Climbing strategy in herbs does not necessarily lead to lower investments into stem biomass. Plant Ecology, 221(11), 1159–1166. https://doi.org/10.1007/s11258-020-01070-9

Landuyt, D., Ampoorter, E., Bastias, C. C., Benavides, R., Müller, S., Scherer-Lorenzen, M., Valladares, F., Wasof, S., & Verheyen, K. (2020a). Importance of overstorey attributes for

understorey litter production and nutrient cycling in European forests. Forest Ecosystems, 7(1), 45. https://doi.org/10.1186/s40663-020-00256-x

Landuyt, D., De Lombaerde, E., Perring, M. P., Hertzog, L. R., Ampoorter, E., Maes, S. L., De Frenne, P., Ma, S., Proesmans, W., Blondeel, H., Sercu, B. K., Wang, B., Wasof, S., & Verheyen, K. (2019). The functional role of temperate forest understorey vegetation in a changing world. Global Change Biology, 25(11), 3625–3641. https://doi.org/10.1111/gcb.14756

Landuyt, D., Maes, S. L., Depauw, L., Ampoorter, E., Blondeel, H., Perring, M. P., Brūmelis, G., Brunet, J., Decocq, G., den Ouden, J., Härdtle, W., Hédl, R., Heinken, T., Heinrichs, S., Jaroszewicz, B., Kirby, K. J., Kopecký, M., Máliš, F., Wulf, M., & Verheyen, K. (2020b). Drivers of above-ground understorey biomass and nutrient stocks in temperate deciduous forests. Journal of Ecology, 108(3), Article 3. https://doi.org/10.1111/1365-2745.13318

Le Duc, M. G., Pakeman, R. J., Putwain, P. D., & Marrs, R. H. (2000). The variable responses of bracken fronds to control treatments in Great Britain. Annals of Botany, 85, 17–29. https://doi.org/10.1006/anbo.1999.1052

Lecomte, X., Bugalho, M. N., Catry, F. X., Fernandes, P. M., Cera, A., & Caldeira, M. C. (2024). Ungulates mitigate the effects of drought and shrub encroachment on the fire hazard of Mediterranean oak woodlands. Ecological Applications, 34(4), e2971. https://doi.org/10.1002/eap.2971

Litton, C. M., Raich, J. W., & Ryan, M. G. (2007). Carbon allocation in forest ecosystems. Global Change Biology, 13(10), 2089–2109. https://doi.org/10.1111/j.1365-2486.2007.01420.x

Liu, R., Yang, X., Gao, R., Hou, X., Huo, L., Huang, Z., & Cornelissen, J. H. C. (2021). Allometry rather than abiotic drivers explains biomass allocation among leaves, stems and roots of Artemisia across a large environmental gradient in China. Journal of Ecology, 109(2), 1026–1040. https://doi.org/10.1111/1365-2745.13532

De Lombaerde, E., Baeten, L., Verheyen, K., Perring, M. P., Ma, S., & Landuyt, D. (2021). Understorey removal effects on tree regeneration in temperate forests: A meta-analysis. Journal of Applied Ecology, 58(1), 9–20. https://doi.org/10.1111/1365-2664.13792

Madgwick, H. A. I. (1965). The weights and nutrient compositions of understorey species in an ashwood. Journal of Ecology, 53(2), 335–341. https://doi.org/10.2307/2257979

Maillard, M., Martin, J.-L., Chollet, S., Catomeris, C., Simon, L., & Grayston, S. J. (2021). Belowground effects of deer in a temperate forest are time-dependent. Forest Ecology and Management, 493, 119228. https://doi.org/10.1016/j.foreco.2021.119228

Mårell, A., Archaux, F., & Korboulewsky, N. (2009). Floral herbivory of the wood anemone (Anemone nemorosa L.) by roe deer (Capreolus capreolus L.). Plant Species Biology, 24(3), 209–214. https://doi.org/10.1111/j.1442-1984.2009.00257.x

Marrs, R. H., & Watt, A. S. (2006). Biological Flora of the British Isles: Pteridium aquilinum (L.) Kuhn. Journal of Ecology, 94(6), 1272–1321. https://doi.org/10.1111/j.1365-2745.2006.01177.x

Monzingo, D. S., Shipley, L. A., Cook, R. C., & Cook, J. G. (2022). Factors influencing predictions of understory vegetation biomass from visual cover estimates. Wildlife Society Bulletin, 46(3), e1300. https://doi.org/10.1002/wsb.1300

Niklas, K. J. (2006). A phyletic perspective on the allometry of plant biomass-partitioning patterns and functionally equivalent organ-categories. New Phytologist, 171(1), 27–40. https://doi.org/10.1111/j.1469-8137.2006.01760.x

Paruelo, J. M., Lauenroth, W. K., & Roset, P. A. (2000). Estimating aboveground plant biomass using a photographic technique. Journal of Range Management, 53(2), 190–193. https://doi.org/10.2307/4003281

Poorter, H., Niinemets, Ü., Ntagkas, N., Siebenkäs, A., Mäenpää, M., Matsubara, S., & Pons, ThijsL. (2019). A meta-analysis of plant responses to light intensity for 70 traits ranging from molecules to whole plant performance. New Phytologist, 223(3), 1073–1105. https://doi.org/10.1111/nph.15754

Poorter, H., Niinemets, Ü., Poorter, L., Wright, I. J., & Villar, R. (2009). Causes and consequences of variation in leaf mass per area (LMA): A meta-analysis. New Phytologist, 182(3), 565–588. https://doi.org/10.1111/j.1469-8137.2009.02830.x

Poorter, H., Niklas, K. J., Reich, P. B., Oleksyn, J., Poot, P., & Mommer, L. (2012). Biomass allocation to leaves, stems and roots: Meta-analyses of interspecific variation and environmental control. New Phytologist, 193(1), 30–50. https://doi.org/10.1111/j.1469-8137.2011.03952.x

Populus, C., Mårell, A., & Korboulewsky, N. (2026). Height, cover and biomass of six common understory species in French temperate forests [Dataset]. Recherche Data Gouv. https://doi.org/10.57745/TEKLCI

Porté, A. J., Samalens, J.-C., Dulhoste, R., Teissier Du Cros, R., Bosc, A., & Meredieu, C. (2009). Using cover measurements to estimate aboveground understorey biomass in Maritime pine stands. Annals of Forest Science, 66(3), Article 3. https://doi.org/10.1051/forest/2009005

Pottier, J., & Jabot, F. (2017). Non-destructive biomass estimation of herbaceous plant individuals: A transferable method between contrasted environments. Ecological Indicators, 72, 769–776. https://doi.org/10.1016/j.ecolind.2016.08.030

Rawlik, M., & Jagodziński, A. M. (2022). Herbaceous layer net primary production of oak-hornbeam forest: Comparing six methods of assessment based on the seasonal dynamics of biomass increments. Ecosystems, 25(2), 337–349. https://doi.org/10.1007/s10021-021-00658-0

Reich, P. B. (2014). The world-wide 'fast–slow' plant economics spectrum: A traits manifesto. Journal of Ecology, 102(2), 275–301. https://doi.org/10.1111/1365-2745.12211

Roth, L., & Streit, B. (2018). Predicting cover crop biomass by lightweight UAS-based RGB and NIR photography: An applied photogrammetric approach. Precision Agriculture, 19(1), 93–114. https://doi.org/10.1007/s11119-017-9501-1

Röttgermann, M., Steinlein, T., Beyschlag, W., & Dietz, H. (2000). Linear relationships between aboveground biomass and plant cover in low open herbaceous vegetation. Journal of Vegetation Science, 11(1), 145–148. https://doi.org/10.2307/3236786

Rue-Johns, A. Z., Crotteau, J. S., D'Amore, D. V., & Barnard, J. C. (2021). Biomass regressions for understory species in young-growth Sitka spruce–western hemlock forests of southeast Alaska. Northwest Science, 95(1), 114–124. https://doi.org/10.3955/046.095.0108

Schmidt, A. F., & Finan, C. (2018). Linear regression and the normality assumption. Journal of Clinical Epidemiology, 98, 146–151. https://doi.org/10.1016/j.jclinepi.2017.12.006

Tackenberg, O. (2007). A new method for non-destructive measurement of biomass, growth rates, vertical biomass distribution and dry matter content based on digital image analysis. Annals of Botany, 99(4), 777–783. https://doi.org/10.1093/aob/mcm009

Taylor, K. (2005). Biological Flora of the British Isles: Rubus vestitus Weihe. Journal of Ecology, 93(6), 1249–1262. https://doi.org/10.1111/j.1365-2745.2005.01076.x

Taylor, K., Rowland, A. P., & Jones, H. E. (2001). Molinia caerulea (L.) Moench. Journal of Ecology, 89(1), 126–144. https://doi.org/10.1046/j.1365-2745.2001.00534.x

Thomas, S. C., Halpern, C. B., Falk, D. A., Liguori, D. A., & Austin, K. A. (1999). Plant diversity in managed forests: Understory responses to thinning and fertilization. Ecological Applications, 9(3), 864–879. https://doi.org/10.1890/1051-0761(1999)009%5B0864:PDIMFU%5D2.0.CO;2

Vernay, A. (Ed.). (2026). Recommendation of: Allometric scaling relationships of biomass for six common understory species in French temperate forests. Round#3. Peer Community in Plants, plants.100072. https://doi.org/10.24072/pci.plants.100072

Warton, D. I., Duursma, R. A., Falster, D. S., & Taskinen, S. (2012). Smatr 3– an R package for estimation and inference about allometric lines. Methods in Ecology and Evolution, 3(2), 257–259. https://doi.org/10.1111/j.2041-210X.2011.00153.x

West, G. B., Brown, J. H., & Enquist, B. J. (1997). A general model for the origin of allometric scaling laws in biology. Science, 276(5309), 122–126. https://doi.org/10.1126/science.276.5309.122

West, G. B., Brown, J. H., & Enquist, B. J. (1999). The fourth dimension of life: Fractal geometry and allometric scaling of organisms. Science, 284(5420), 1677–1679. https://doi.org/10.1126/science.284.5420.1677

Wickham, H. (2023). modelr: Modelling functions that work with the pipe (p. 0.1.11). https://doi.org/10.32614/CRAN.package.modelr

Wright, I. J., Reich, P. B., Westoby, M., Ackerly, D. D., Baruch, Z., Bongers, F., Cavender-Bares, J., Chapin, T., Cornelissen, J. H. C., Diemer, M., Flexas, J., Garnier, E., Groom, P. K., Gulias, J., Hikosaka, K., Lamont, B. B., Lee, T., Lee, W., Lusk, C., … Villar, R. (2004). The worldwide leaf economics spectrum. Nature, 428(6985), 821–827. https://doi.org/10.1038/nature02403